J|A|C|S COMMUNICATIONS

Published on Web 03/05/2009

Metal Nanoparticles Functionalized with Molecular and Supramolecular Switches

Rafal Klajn,[†,‡] Lei Fang,[‡] Ali Coskun,[‡] Mark A. Olson,[‡] Paul J. Wesson,[†] J. Fraser Stoddart,*[,‡] and Bartosz A. Grzybowski*[,†,‡]

Department of Chemical and Biological Engineering and Department of Chemistry, Northwestern University, 2145 Sheridan Road, Evanston, Illinois 60208-3113

Received January 13, 2009; E-mail: stoddart@northwestern.edu; grzybor@northwestern.edu

The advent of mechanically interlocked molecules (MIMs), such as catenanes and rotaxanes,[1] has contributed significantly to the development of tunable molecular architectures on scales from the molecular[2] to the nanoscopic.[3] Highly programmable and efficient syntheses of bistable catenanes and rotaxanes[1] employing template-directed protocols[4] enable the introduction of bistability,[5] a prerequisite for the operation of molecular switches and machines[6] having potential uses in molecular electronic devices (MEDs),[7] molecular switch tunnel junctions (MSTJs),[8] mechanized mesoporous silica nanoparticles (MMSNPs)[9] for drug delivery, and nanoelectromechanical systems (NEMS).[10]

Despite these achievements, the challenge that remains for these bistable molecules is their incorporation into integrated nanosystems. The first step in this direction is the conjugation of the MIMs with nanoscopic building blocks, such as metal nanoparticles (MNPs), which display a range of novel optical,[11] electronic,[12] catalytic,[13] and mechanical[14] properties. Traditional methods[15] of MNP functionalization are based on the use of thiolate ligands in a reducing environment; such conditions are not compatible with a wide range of functional groups[16] in molecules including bistable donor−acceptor catenanes and rotaxanes.[5] Herein, we describe an alternative strategy for the preparation of functionalized MNPs with a variety of cores (Au, Pt, Pd) using weakly protected MNP "precursors" and dithiolanes terminated in either redox-active MIM components, such as tetrathiafulvalene (TTF), or actual MIMs, such as a bistable [2]catenane. Characterization of these nanostructures by transmission electron microscopy (TEM), ζ-potential measurements, and cyclic voltammetry (CV) confirms that the "switches" retain their activity when attached to the NPs. At the same time, the oxidation potentials of the adsorbed switches depend on and can be modulated (up to a factor of 2) by their surface fraction on the MNP surfaces. These experimental results suggest the presence of cooperative effects within the MIM monolayer and can be rationalized in terms of electrostatic arguments based on the Poisson−Boltzmann equation describing electric potentials around the switchable particles.

The redox-active ligand **2** incorporating TTF was obtained in 41% yield by esterification of a known[17] TTF derivative with (±)-thioctic acid [see the Supporting Information (SI)]. The bistable [2]catenane **3**·4PF_6, terminated in its side chain with a dithiolane ring, was made in 26% yield by employing a macrocyclic polyether[2] incorporating TTF and 1,5-dioxynaphthalene (DNP) units as the template for the formation of the mechanically interlocked cyclobis(paraquat-*p*-phenylene) ($CBPQT^{4+}$) ring at room temperature in DMF under ultrahigh (15 kbar) pressure (see the SI).

The functionalized MNPs (M = Au, Pt, Pd) were prepared from "precursor" MNPs stabilized with low-affinity ligands, namely, tetraoctylammonium bromide (TOAB).[18] These precursors were prepared by reducing PhMe solutions of tetraoctylammonium tetrachloroaurate $[AuCl_4]^-$, tetrachloroplatinate $[PtCl_4]^{2-}$, and tetrachloropalladate $[PdCl_4]^{2-}$, respectively, with aqueous solutions of $NaBH_4$. TEM images of AuNPs, PtNPs, and PdNPs (Figure 1)

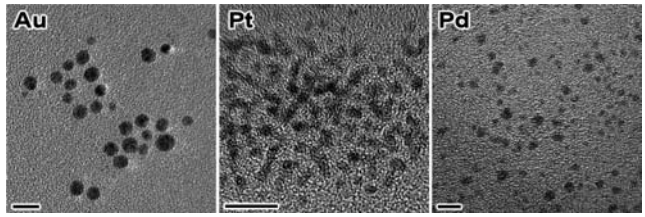

Figure 1. TEM images of the (left) gold, (center) platinum, and (right) palladium "precursor" MNPs. Scale bars correspond to 10 nm.

revealed that the particles have the following diameters: $d_{AuNPs} = 4.58 \pm 1.23$ nm, $d_{PtNPs} = 2.36 \pm 0.64$ nm, and $d_{PdNPs} = 2.72 \pm 0.27$ nm. Although these MNPs display only short-term stability, they undergo rapid ligand-exchange reactions (Figure 2a) when mixed as solutions in PhMe with excesses of dithiolane ligands dissolved in MeCN.

In order to ensure good solubilities of modified MNPs in solvents (e.g., MeCN) suitable for reversible redox chemistry on donor−acceptor MIMs and their supramolecular precursors, we prepared MNPs covered with *mixed* self-assembled monolayers (*m*SAMs) comprising functional ligands **2** or $\mathbf{3}^{4+}$ and various "inert" background ligands. Ultimately, we found that **1** (Figure 2b) was the background ligand of choice and rendered the **1**/**2**-MNPs and **1**/$\mathbf{3}^{4+}$-MNPs readily soluble in MeOH [for fractional coverages (χ)[18e,19] of $\mathbf{2}^{2+}$ and **3** in the monolayer of $\chi_{\mathbf{2}} \leq 0.30$ and $\chi_{\mathbf{3}^{4+}} \leq 0.20$], MeCN ($\chi_{\mathbf{2}} \leq 0.25$, $\chi_{\mathbf{3}^{4+}} \leq 0.20$), and DMF ($\chi_{\mathbf{2}} \leq 1.0$, $\chi_{\mathbf{3}^{4+}} \leq 0.50$).

A qualitative manifestation of the ligands' presence on the MNP surfaces was a drastic change in the solubility of the MNPs. Prior to ligand exchange, the TOAB-protected MNPs were soluble only in strongly oleophilic solvents, such as PhMe or hexane. After functionalization with **1**/$\mathbf{3}^{4+}$ or **1**/**2**, however, they precipitated from PhMe solutions (either spontaneously or after the addition of hexane) but were readily soluble in more polar solvents, such as MeOH, MeCN, and DMF.

Next, we investigated changes in the surface and ζ potentials[20] of both **1**/**2**-MNPs and **1**/$\mathbf{3}^{4+}$-MNPs as a function of the redox potential. Figure 3 illustrates the results of these experiments for the case of AuNPs (the trends recorded for PdNPs and PtNPs were similar). When subjected to $Fe(ClO_4)_3$ oxidation, **1**/**2**-AuNPs ($\chi_{TTF} = 0.25$) (1 in Figure 3a,b) were oxidized to **1**/$\mathbf{2}^{2+}$-AuNPs (2 in

[†] Department of Chemical and Biological Engineering.
[‡] Department of Chemistry.

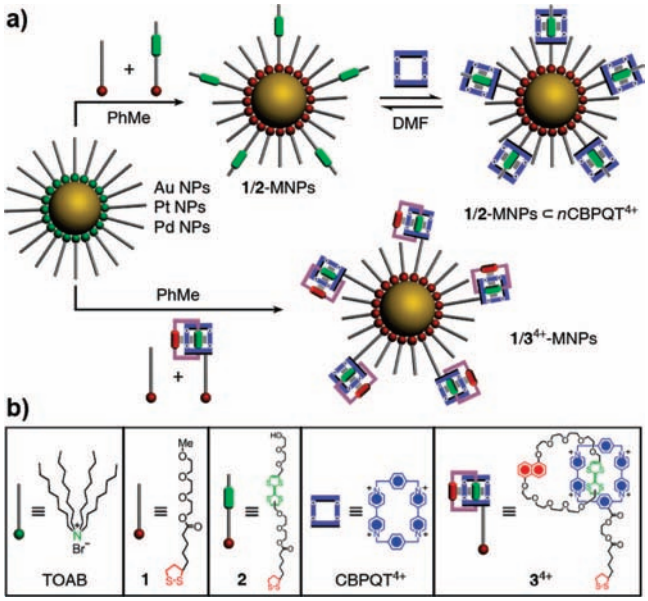

Figure 2. Functionalization of weakly protected NPs. (a) TOAB-protected Au, Pt, or Pd NPs undergo facile ligand exchange when mixed with dithiolanes: (top) Preparation of TTF-functionalized NPs (**1/2**-MNPs) and the formation of the pseudorotaxane complex **1/2**-MNPs⊂*n*CBPQT^{4+} on the NP surface. (bottom) Preparation of catenane-functionalized NPs **1/3**$^{4+}$-MNPs. (b) Structural formulas of TOAB, dithiolane-functionalized triethylene glycol **1** and TTF **2**, CBPQT^{4+}, and the dithiolane-functionalized catenane **3**$^{4+}$ (green station = TTF; red station = DNP). The counterions in **3**$^{4+}$ are four PF_6^- ions.

Figure 3a,b) and had a ζ potential of $+21.9 \pm 1.9$ mV in DMF. Upon addition of ascorbic acid, the TTF^{2+} was reduced back to the neutral state, and the ζ potential of the particles was close to zero (-0.5 ± 2.1 mV). The MNPs underwent several (more than five) oxidation/reduction cycles between the same values of the ζ potential. To confirm the ability of **2** to form pseudorotaxanes with π-electron-deficient CBPQT^{4+} rings on the surface of MNPs, we introduced an excess amount of CBPQT·4PF_6 to the solution of **1/2**-AuNPs and observed that the ζ potential increased to $+29.2 \pm 0.7$ mV. This increase in the ζ potential was commensurate with

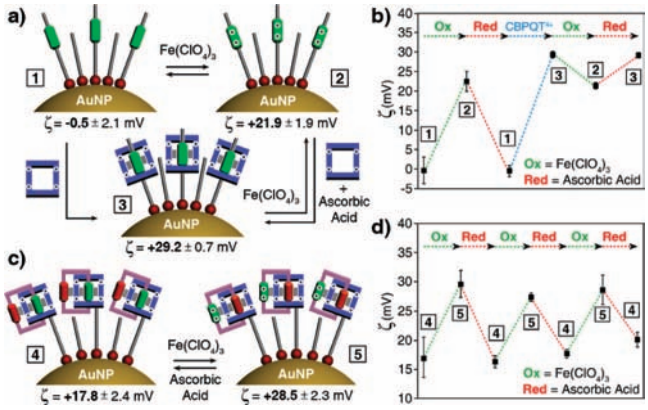

Figure 3. ζ Potential measurements on (a, b) **1/2**-AuNPs and (c, d) **1/3**$^{4+}$-AuNPs. (a) Reversible transformations and ζ potential values of (1) **1/2**-AuNPs, (2) their oxidized form, **1/2**$^{2+}$-AuNPs, and (3) the pseudorotaxane complex **1/2**-AuNPs⊂*n*CBPQT^{4+}. (b) Changes in ζ potential for **1/2**-AuNPs as a function of oxidation/reduction [Ox = addition of $Fe(ClO_4)_3$; Red = addition of ascorbic acid] and reversible formation of a pseudorotaxane. (c) Reversible transformations and ζ potential values for (4) **1/3**$^{4+}$-AuNPs and (5) their oxidized form, **1/3**$^{6+}$-AuNPs. (d) Changes in ζ potential for **1/3**$^{4+}$-AuNPs (black squares) as a function of reduction/oxidation processes.

the formation of positively charged pseudorotaxanes on the surface of AuNPs [**1/2**-AuNPs⊂*n*CBPQT^{4+}, where "⊂" denotes threading of CBPQT^{4+} onto **2** (3 in Figure 3a,b)]. As expected, addition of $Fe(ClO_4)_3$ led to a *decrease* in the ζ potential with respect to the value observed for **1/2**$^{2+}$-AuNPs. This decrease can be attributed to the dissociation of the pseudorotaxane (Figure 3a,b) driven by the electrostatic repulsion between TTF^{2+} and CBPQT^{4+}. To further confirm that the changes in the ζ potential originated from the reversible redox chemistry and specific threading on the surface of the NPs, we carried out control experiments using NPs covered with **1** only (i.e., **1**-AuNPs). The ζ potential of these particles was close to zero and was not affected by the addition of $Fe(ClO_4)_3$, ascorbic acid, or CBPQT·4PF_6.

Similarly, the ζ potential of the catenane-functionalized **1/3**$^{4+}$-AuNPs ($\chi_{3^{4+}} = 0.50$) in DMF could be switched reversibly between the values $+17.8 \pm 2.4$ and $+28.5 \pm 2.3$ mV upon sequential addition of $Fe(ClO_4)_3$ and ascorbic acid (Figure 3c,d). This reversible increase in ζ potential by a factor of $\sim$1.5 agrees well with the oxidation of **3**$^{4+}$ to **3**$^{6+}$ and the formation of the species labeled 4 and 5, respectively, in Figure 3c,d. In the control experiments, we investigated AuNPs ($\chi = 0.50$) functionalized with a degenerate catenane (see the SI). In contrast to **1/3**$^{4+}$-AuNPs, the ζ potential of these particles did not change upon the addition of $Fe(ClO_4)_3$ or ascorbic acid (see the SI).

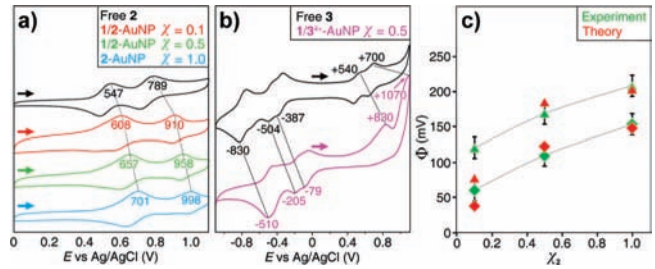

Figure 4. CV of (a) free **2** (black) and **1/2**-AuNPs with $\chi_2 = 0.1$ (red), 0.5 (green), and 1.0 (blue). (b) CV of free **3**·4PF_6 (black) and **1/3**$^{4+}$-AuNPs with $\chi_{3^{4+}} = 0.50$ (pink). (c) Experimental (green) and theoretical (red) values for the oxidation-peak shifts of **2** for both the first (**2** → **2**$^{+\bullet}$, ◆) and second (**2**$^{+\bullet}$ → **2**$^{2+}$, ▲) oxidations.

The presence and switching of both **2** and **3**$^{4+}$ on the MNPs was further studied by CV (Figure 4a,b). CV measurements on free **2** and **3**$^{4+}$ as well as on **1/2**-AuNPs and **1/3**$^{4+}$-AuNPs were carried out in an electrolyte solution in DMF ($LiClO_4$, $c = 0.05$ M, 298 K). Oxidation peaks of **1/2**-AuNPs corresponding to TTF → TTF$^{+\bullet}$ (+608, +657, and +701 mV for $\chi = 0.1$, 0.5, and 1.0, respectively) and TTF$^{+\bullet}$ → TTF^{2+} (+910, +958, and +998 mV for $\chi = 0.1$, 0.5, and 1.0, respectively) were observed at redox potentials more positive than those for free **2** (+547 and +789 mV). Likewise, CV of **3**$^{4+}$ and **1/3**$^{4+}$-AuNPs ($\chi = 0.5$) showed the same set of peaks (Figure 4b), with both the oxidation and reduction peaks of the **1/3**$^{4+}$-AuNPs shifted to more positive values.

The shift in the oxidation potential for **1/2**-AuNPs and its dependence on the surface coverage of **2** (χ_2) can be explained using electrostatic arguments. The oxidation of adsorbed **2** (either **2** → **2**$^{+\bullet}$ or **2**$^{+\bullet}$ → **2**$^{2+}$) on the surface of **1/2**-AuNPs results in an increase in the electrostatic potential, Φ, at the particle's surface. Importantly, the more **2**$^{2+}$ there is on the surface, the more difficult it is to oxidize more of these groups and introduce additional charge onto the particle (negative electrostatic cooperativity). Therefore, we expect the oxidation potential of adsorbed **2** to depend on Φ: to a first approximation, one can write $E^x = E^0 + \Phi$, where E^x is the observed oxidation potential at the particle's surface (metal core plus SAM) and E^0 is the oxidation potential of **2** in a dilute solution.

To estimate the magnitude of the ζ potential and the effects of the surface coverage on the MIM oxidation potential, we solved the linearized Poisson−Boltzmann equation $\nabla^2\Phi = \kappa^2\Phi$, where κ^{-1} is the Debye screening length (see section 5 in the SI). The boundary conditions were $\Phi(\infty) = 0$ and $\partial\Phi/\partial r|_{r=a} = -\sigma/\varepsilon_0\varepsilon$, where ε_0 is the permittivity of free space, $\varepsilon = 38.25$ is the dielectric constant of DMF, σ is the surface charge density, and a is the radius of the particle (core plus SAM). Here we calculated σ using a "charge-regulating" boundary condition,[21] which accounts for the equilibrium between $\mathbf{2}^{+\bullet}$, $\mathbf{2}^{2+}$, and ClO_4^- in solution and the three associated species $\mathbf{2}^{+\bullet}\cdot ClO_4^-$, $\mathbf{2}^{2+}\cdot ClO_4^-$, and $\mathbf{2}^{2+}\cdot 2ClO_4^-$. The equilibrium constants for the counterion adsorption are of the form $K^x = c\ \exp(-e\Phi/k_BT) = [2^x][ClO_4^-]/[2^x\cdot ClO_4^-]$, where the superscript x denotes the oxidation state of **2**, c is the dissociation constant in the absence of an electric field, and the exponential term accounts for the energetic cost of introducing an additional charge onto a charged particle of potential Φ. We then calculated the surface potential Φ for two cases: (*i*) all adsorbed **2** has been oxidized to $\mathbf{2}^{+\bullet}$ and (*ii*) all adsorbed **2** has been oxidized to $\mathbf{2}^{2+}$, corresponding to the states at the first and the second oxidation peaks, respectively (see the SI for more details). Figure 4c shows that these calculated potentials agree well with the magnitudes and directions of the oxidation-peak shifts for the two oxidation states of **2**. Analogous reasoning can be extended to $\mathbf{1}/\mathbf{3}^{4+}$-MNPs, where both the TTF oxidation peaks and $CBPQT^{4+}$ reduction peaks were observed at values more positive than those for free $\mathbf{3}^{4+}$ (Figure 4b).

In summary, a methodology for attaching chemically sensitive functional groups to the surface of metal nanoparticles was developed and used to prepare a variety (i.e., Au, Pt, Pd) of NPs functionalized with thread-containing, π-electron-rich recognition sites as well as with bistable [2]catenanes. On-nanoparticle redox switching of these groups and threading/dethreading of an electron-deficient macrocycle onto MNPs decorated with electron-rich stalks were verified by ζ potential measurements and CV. These findings, including the observation that the redox potentials of the "switches" can be regulated by the composition of the *m*SAMs, underlie the potential development of "tunable" NP components that may be useful in the assembly of responsive, nanostructured materials.[22]

Acknowledgment. This research was supported by the Microelectronics Advanced Research Corporation (MARCO) and its Center on Functional Engineered Nano Architectonics (FENA). B.A.G. gratefully acknowledges financial support from the Alfred P. Sloan Fellowship and the Dreyfus Teacher−Scholar Award. R.K. was supported by the National Science Foundation under the Northwestern MRSEC. We thank Dr. Ali Trabolsi for helpful discussions.

Supporting Information Available: Experimental details and spectral characterization data. This material is available free of charge via the Internet at http://pubs.acs.org.

References

(1) (a) Breault, G. A.; Hunter, C. A.; Mayers, P. C. *Tetrahedron* **1999**, *55*, 5265–5293. (b) Fujita, M. *Acc. Chem. Res.* **1999**, *32*, 53–61. (c) Hubin, T. J.; Busch, D. H. *Coord. Chem. Rev.* **2000**, *200*, 5–52. (d) Stoddart, J. F.; Colquhoun, H. M. *Tetrahedron* **2008**, *64*, 8231–8263.

(2) Asakawa, M.; Ashton, P. R.; Balzani, V.; Credi, A.; Hamers, C.; Mattersteig, G.; Montalti, M.; Shipway, A. N.; Spencer, N.; Stoddart, J. F.; Tolley, M. S.; Venturi, M.; White, A. J. P.; Williams, D. J. *Angew. Chem., Int. Ed.* **1998**, *37*, 333–337.

(3) (a) Saha, S.; Leung, K. C.-F.; Nguyen, T. D.; Stoddart, J. F.; Zink, J. I. *Adv. Funct. Mater.* **2007**, *17*, 685–693. (b) Olson, M. A.; Braunschweig, A. B.; Fang, L.; Ikeda, T.; Klajn, R.; Trabolsi, A.; Wesson, P. J.; Benítez, D.; Mirkin, C. A.; Grzybowski, B. A.; Stoddart, J. F. *Angew. Chem. Int. Ed.* **2009**, *48*, 1792–1797.

(4) (a) Anderson, S.; Anderson, H. L.; Sanders, J. K. M. *Acc. Chem. Res.* **1993**, *26*, 469–475. (b) Blanco, M. J.; Chambron, J. C.; Jiménez, M. C.; Sauvage, J.-P. *Top. Stereochem.* **2003**, *23*, 125–173. (c) Vickers, M. S.; Beer, P. D. *Chem. Soc. Rev.* **2007**, *36*, 211–225.

(5) (a) Ashton, P. R.; Ballardini, R.; Balzani, V.; Baxter, I.; Credi, A.; Fyfe, M. C. T.; Gandolfi, M. T.; Gómez-López, M.; Martínez-Díaz, M. V.; Piersanti, A.; Spencer, N.; Stoddart, J. F.; Venturi, M.; White, A. J. P.; Williams, D. J. *J. Am. Chem. Soc.* **1998**, *120*, 11932–11942. (b) Jeppesen, J. O.; Perkins, J.; Becher, J.; Stoddart, J. F. *Angew. Chem., Int. Ed.* **2001**, *40*, 1216–1217. (c) Kay, E. R.; Leigh, D. A.; Zerbetto, F. *Angew. Chem., Int. Ed.* **2007**, *46*, 72–191.

(6) Balzani, V.; Credi, A.; Venturi, M. *Molecular Devices and Machines*; Wiley-VCH: Weinheim, Germany, 2006.

(7) Green, J. E.; Choi, J. W.; Boukai, A.; Bunimovich, Y.; Johnston-Halperin, E.; DeIonno, E.; Luo, Y.; Sheriff, B. A.; Xu, K.; Shin, Y. S.; Tseng, H.-R.; Stoddart, J. F.; Heath, J. R. *Nature* **2007**, *445*, 414–417.

(8) (a) Wong, E. W.; Collier, C. P.; Behloradsky, M.; Raymo, F. M.; Stoddart, J. F.; Heath, J. R. *J. Am. Chem. Soc.* **2000**, *122*, 5831–5840. (b) Collier, C. P.; Mattersteig, G.; Wong, E. W.; Luo, Y.; Beverly, K.; Sampaio, J.; Raymo, F. M.; Stoddart, J. F.; Heath, J. R. *Science* **2000**, *289*, 1172–1175.

(9) (a) Patel, K.; Angelos, S.; Dichtel, W. R.; Coskun, A.; Yang, Y. W.; Zink, J. I.; Stoddart, J. F. *J. Am. Chem. Soc.* **2008**, *130*, 2382–2383.

(10) (a) Berna, J.; Leigh, D. A.; Lubomska, M.; Mendoza, S. M.; Perez, E. M.; Rudolf, P.; Teobaldi, G.; Zerbetto, F. *Nat. Mater.* **2005**, *4*, 704–710. (b) Liu, Y.; Flood, A. H.; Bonvallet, P. A.; Vignon, S. A.; Northrop, B. H.; Tseng, H.-R.; Jeppesen, J. O.; Huang, T. J.; Brough, B.; Baller, M.; Magonov, S.; Solares, S. D.; Goddard, W. A.; Ho, C. M.; Stoddart, J. F. *J. Am. Chem. Soc.* **2005**, *127*, 9745–9759.

(11) (a) Kalsin, A. M.; Pinchuk, A. O.; Smoukov, S. K.; Paszewski, M.; Schatz, G. C.; Grzybowski, B. A. *Nano Lett.* **2006**, *6*, 1896–1903. (b) Pinchuk, A. O.; Kalsin, A. M.; Kowalczyk, B.; Schatz, G. C.; Grzybowski, B. A. *J. Phys. Chem. C* **2007**, *111*, 11816–11822.

(12) (a) McConnell, W. P.; Novak, J. P.; Brousseau, L. C.; Fuierer, R. R.; Tenent, R. C.; Feldheim, D. L. *J. Phys. Chem. B* **2000**, *104*, 8925–8930. (b) Nitzan, A.; Ratner, M. A. *Science* **2003**, *300*, 1384–1389.

(13) (a) Tian, N.; Zhou, Z. Y.; Sun, S. G.; Ding, Y.; Wang, Z. L. *Science* **2007**, *316*, 732–735. (b) Park, J. Y.; Zhang, Y.; Grass, M.; Zhang, T.; Somorjai, G. A. *Nano Lett.* **2008**, *8*, 673–677.

(14) Klajn, R.; Bishop, K. J. M.; Fialkowski, M.; Paszewski, M.; Campbell, C. J.; Gray, T. P.; Grzybowski, B. A. *Science* **2007**, *316*, 261–264.

(15) (a) Brust, M.; Walker, M.; Bethell, D.; Schiffrin, D. J.; Whyman, R. *Chem. Commun.* **1994**, 801–802. (b) Fitzmaurice, D.; Rao, S. N.; Preece, J. A.; Stoddart, J. F.; Wenger, S.; Zaccheroni, N. *Angew. Chem., Int. Ed.* **1999**, *38*, 1147–1150.

(16) Witt, D.; Klajn, R.; Barski, P.; Grzybowski, B. A. *Curr. Org. Chem.* **2004**, *8*, 1763–1797.

(17) Tseng, H.-R.; Vignon, S. A.; Celestre, P. C.; Perkins, J.; Jeppesen, J. O.; Di Fabio, A.; Ballardini, R.; Gandolfi, M. T.; Venturi, M.; Balzani, V.; Stoddart, J. F. *Chem.—Eur. J.* **2004**, *10*, 155–172.

(18) (a) Abad, J. M.; Mertens, S. F. L.; Pita, M.; Fernandez, V. M.; Schiffrin, D. J. *J. Am. Chem. Soc.* **2005**, *127*, 5689–5694. (b) Zhang, G. X.; Zhang, D. Q.; Zhao, X. H.; Ai, X. C.; Zhang, J. P.; Zhu, D. B. *Chem.—Eur. J.* **2006**, *12*, 1067–1073. (c) van Herrikhuyzen, J.; Janssen, R. A. J.; Meijer, E. W.; Meskers, S. C. J.; Schenning, A. *J. Am. Chem. Soc.* **2006**, *128*, 686–687. (d) We verified that dodecylamine- or undecanethiol-protected MNPs do not undergo a facile ligand exchange reaction with dithiolanes. Rather, they precipitate from the solution after prolonged periods of time to yield insoluble solids. (e) We also verified by TEM and UV−vis spectroscopy that the functionalization procedure does not affect the size distribution, shape, or optical properties of the MNPs.

(19) The fractional coverage, χ, was calculated on the basis of the ratio of ligands in the solution used for functionalization of the MNPs. We verified by chronocoulometry experiments (see the SI) that the ratio of ligands **1** and L (L = **2**, $\mathbf{3}^{4+}$) in the MNP functionalization solution is proportional to the ratio of the ligands on the resulting MNPs (i.e., dithiolanes **1** and L adsorb onto the surface of MNPs at equal rates). Details of these studies will be published separately.

(20) (a) Sylvestre, J. P.; Kabashin, A. V.; Sacher, E.; Meunier, M.; Luong, J. H. T. *J. Am. Chem. Soc.* **2004**, *126*, 7176–7177. (b) You, C. C.; De, M.; Han, G.; Rotello, V. M. *J. Am. Chem. Soc.* **2005**, *127*, 12873–12881. (c) Kalsin, A. M.; Kowalczyk, B.; Smoukov, S. K.; Klajn, R.; Grzybowski, B. A. *J. Am. Chem. Soc.* **2006**, *128*, 15046–15047.

(21) (a) Carnie, S. L.; Chan, D. Y. C.; Gunning, J. S. *Langmuir* **1994**, *10*, 2993–3009. (b) Bishop, K. J. M.; Grzybowski, B. A. *ChemPhysChem* **2007**, *8*, 2171–2176.

(22) Klajn, R.; Bishop, K. J. M.; Grzybowski, B. A. *Proc. Natl. Acad. Sci. U.S.A.* **2007**, *104*, 10305–10309.

JA9001585